Exploring the mechanism of *Schisandra rubriflora* in the treatment of polycystic ovary syndrome based on network pharmacology and molecular docking

Zhengyan Dou[1], Qingxian Li[2*], Jing Zhang[3] and Xin Zhang[2]

Abstract

Background Polycystic ovary syndrome (PCOS) is an endocrine disease associated with reproductive and metabolic abnormalities. The aim of this study was to elucidate the effects of *Schisandra rubriflora* (*S. rubriflora*) on PCOS and its related mechanisms using network pharmacology, molecular docking and in vitro experiments.

Materials and methods HERB database and SwissTargetPrediction database were used to obtain the active components and the targets of *S. rubriflora*. Differentially expressed genes (DEGs) associated with PCOS were obtained by analyzing GSE54248 dataset. A protein-protein interaction network was constructed, and topological analyses were performed to identify the hub targets and main bioactive components. The binding abilities between hub targets and key components were studied by molecular docking. Finally, in vitro PCOS models were constructed with KGN cells and rat ovarian granulosa cells, respectively, and the regulatory effects of schisandrin, a key bioactive component of *S. rubriflora*, on the cells were investigated by in vitro assays.

Results A total of 14 bioactive ingredients of *S. rubriflora* and 26 potential therapeutic targets of *S. rubriflora* in PCOS treatment were obtained. Bioinformatics analyses suggested that the mechanisms of *S. rubriflora* in treating PCOS were related to IL-17 signaling pathway and TNF signaling pathway. The binding affinities between key components of *S. rubriflora* (schisandrin, wyerone, and rugosal) and hub targets (PTGS2, MMP9, MCL1, and JUN) were high. Schisandrin could attenuate lipopolysaccharide-induced inflammation, oxidative stress, and apoptosis of KGN cells and rat ovarian granulosa cells, as well as inhibit hub target expression and TNF pathway activation.

Conclusion PTGS2, MMP9, MCL1 and JUN are potential targets for *S. rubriflora* to treat PCOS. Schisandrin, a main component of *S. rubriflora*, may be a candidate for the treatment of PCOS.

Keywords Polycystic ovary syndrome, *S. Rubriflora*, Network pharmacology, Schisandrin, Ovarian granulosa cells
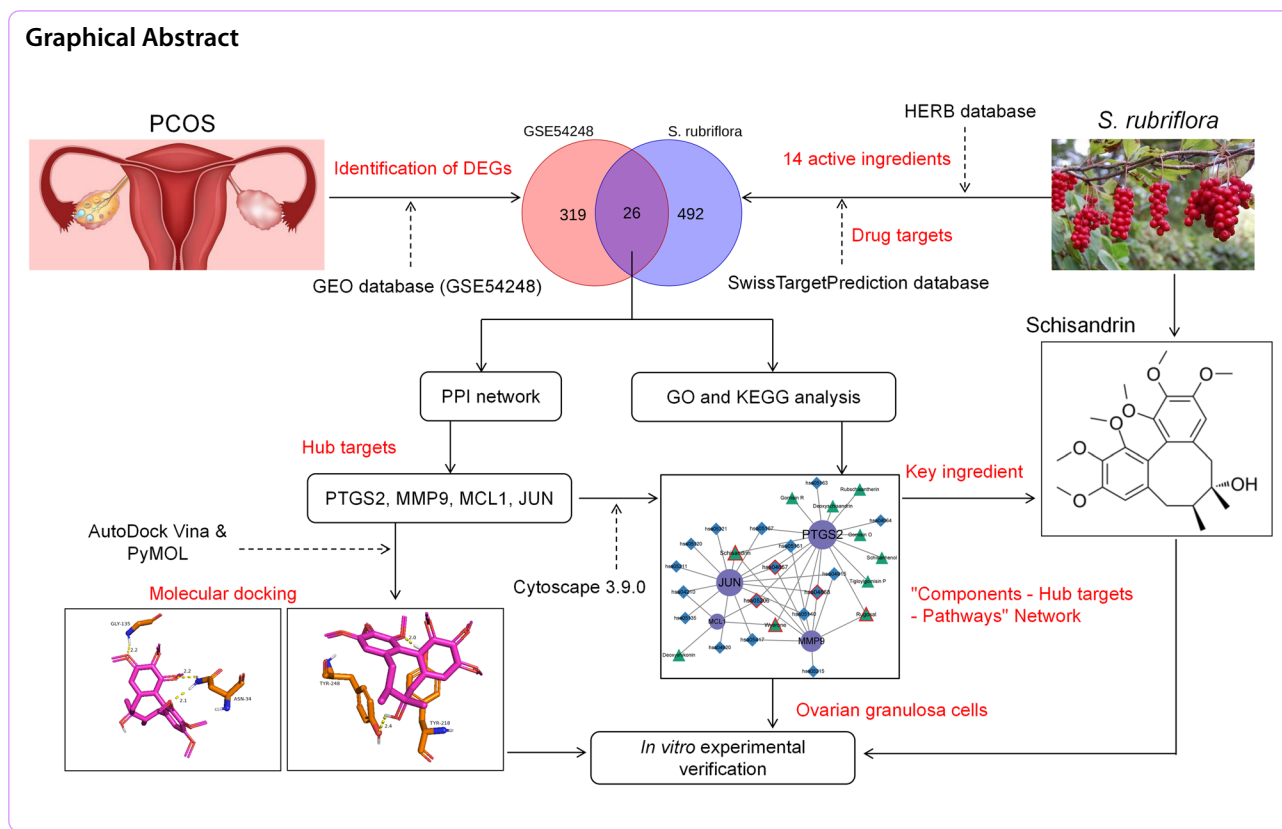
*Correspondence:
Qingxian Li
Kxliqx@163.com
Full list of author information is available at the end of the article

Dou *et al. Journal of Ovarian Research*   (2025) 18:16

Page 2 of 20

Graphical Abstract

Introduction

Polycystic ovary syndrome (PCOS) is a prevalent and intricate endocrine and metabolic disorder, representing one of the most frequent causes of female infertility, affecting up to 15% of women of childbearing age worldwide [1, 2]. PCOS leads to serious complications such as disruption of gonadotropin secretion, increased androgen production, chronic anovulation and polycystic ovary morphology, often accompanied by insulin resistance and obesity [3–5]. Although the exact cause of PCOS remains unknown, genetic factors along with epigenetic changes as well as environmental and behavioral variables are all associated with its pathogenesis [6]. Currently treatments for PCOS include oral contraceptives, antiandrogens, insulin sensitizers and ovulation stimulating drugs; however these strategies have certain limitations such as higher recurrence rate and high incidence of side effects [7].

Some phytochemicals derived from herbs in traditional Chinese medicine (TCM) are promising to ameliorate various symptoms associated with PCOS including insulin resistance, hyperinsulinemia, hyperandrogenemia, abnormal ovarian function, obesity, abortion, infertility, etc [8, 9]. *Schisandra rubriflora* (*S. rubriflora*), a woody vine native to western Sichuan Province in China, is used in TCM to treat hepatitis, chronic gastroenteritis and neurasthenia [10, 11]. Lignans, especially dibenzocyclooctadiene lignans (DBCLS), nortriterpenoids and dinortriterpenoids are considered to be the main metabolites of *S. rubriflora* [12]. DBCLS has been reported to be active in inhibiting the replication of human immunodeficiency virus [13]. Extracts from the branches of *S. rubriflora* can effectively reduce the level of glutamino-pyruvate transaminase in the blood, which may help in the treatment of liver and bile duct diseases [14]. In addition, leaf, fruit and shoot extracts of S. rubriflora can also effectively inhibit the activity of pro-inflammatory cyclooxygenase 1 and 2, 15-lipoxygenase, and phospholipase A2, which suggests its anti-inflammatory effect [15]. However, the potential therapeutic mechanism of *S. rubriflora* for PCOS remains unclear.

Network pharmacology has wide application within TCM research providing new ideas for molecular pharmacological mechanism [16, 17]. Molecular docking serves as a tool capable of predicting receptor-ligand complex binding modes [18]. This study aims at utilizing network pharmacology and molecular docking techniques to explore targets and potential mechanisms underlying S.rubriflora's treatment efficacy against

Dou *et al. Journal of Ovarian Research*   (2025) 18:16

Page 3 of 20

PCOS, thereby laying down theoretical groundwork for its clinical applications.

Methods and materials

Screening of the targets of *S. Rubriflora* in PCOS treatment

The active ingredients of *S. rubriflora* were obtained from the HERB database (http://herb.ac.cn/). From the PubChem database (https://pubchem.ncbi.nlm.nih.gov), the chemical structures and SMILES files of the ingredients were obtained. SMILES files were imported into SwissTargetPrediction database (http://www.swisstargetprediction.ch), to obtain the drug targets [19]. From Gene Expression Omnibus (GEO) database (https://www.ncbi.nlm.nih.gov/gds/), the data of GSE54248 and GSE34526 were downloaded. GSE54248 contains the gene expression profile of peripheral blood samples of 4 patients with PCOS and of 4 cases of control subjects. With $P < 0.05$ and |log2 fold change|>1 as the thresholds, differential expression was analyzed by GEO2R online tool, and differentially expressed genes (DEGs) were obtained. GSE34526 contains the gene expression profile of ovarian granulosa cells of women with PCOS and healthy controls, which was used to investigate the expression characteristics of hub targets of *S. rubriflora* in granulosa cells. BioLadder online platform (http://www.bioinformatics.com.cn/static/others/jvenn/example.html) was applied to draw a Venn diagram based on the DEGs and *S. rubriflora*'s targets, and the therapeutic targets of *S. rubriflora* in PCOS treatment were obtained. Gene ontology (GO) analysis and Kyoto Encyclopedia of Genes and Genomes (KEGG) pathway enrichment analysis of these targets were performed using the clusterProfiler package of R software.

Construction and analysis of protein-protein interaction (PPI) network

The targets were imported into the STRING database (https://cn.string-db.org/) for PPI network construction and analysis. "Species" was set to "*homo sapiens*", and the required minimum interaction score was set to "medium confidence (0.4)", and other parameters were left at their default settings. MCODE plug-in was used to perform module analysis of the target proteins in the PPI network according to the default parameters. The default parameters were: degree cutoff=2, node score cutoff=0.2, K-score=2, and max depth=100.

Identification of hub targets

Using CytoHubba plugin, based on different topological algorithms including betweenness, closeness, degree, edge percolated component (EPC), density of maximum neighborhood component (DMNC), maximal clique centrality (MCC) and maximum neighborhood component (MNC), the PPI network was analyzed. The top 10 targets identified by each algorithm were obtained, and the intersection was taken using UpSet R package, and the hub targets were finally obtained. In addition, the GeneMANIA database (http://genemania.org/) was used to construct the interaction network of hub targets.

Construction of a "component-hub target-pathway" network

The active ingredient of *S. rubriflora*, its targets in PCOS treatment, and the top 20 KEGG pathways were imported into Cytoscape 3.9.0 software to construct the "component-hub target-pathway" network. The degree values of network nodes were analyzed by CytoNCA plug-in to screen out the key components and signaling pathways of *S. rubriflora* in PCOS treatment. Pathview R package was used to color the targets on the key signaling pathways.

Molecular docking

From PubChem (https://pubchem.ncbi.nlm.nih.gov/), the 3D chemical structures of the key components were downloaded, and saved as SDF format. It was then converted to mol2 format by the OpenBabel software (version 3.1.1). From the Protein Data Bank (PDB; https://www.rcsb.org/), X-ray crystal structures of the hub targets were downloaded. All proteins ("receptor") and components ("ligands") files were converted to pdbqt files using AutoDockTools software (version 1.5.7). Molecular docking analysis was performed with AutoDock Vina (version 1.1.2) to evaluate the binding abilities between key components and hub targets. When the binding energy was less than 0, it was considered that proteins and components could spontaneously bind and interact with each other [20]. Finally, PyMOL software was used to visualize the docking results.

Cell culture and treatment

Ovarian granular cells KGN was purchased from Shanghai Yaji Biotechnology Co., Ltd. (Shanghai, China). Rat ovarian granulosa cells were purchased from Procell Biotech (Wuhan, China). The cells were cultured in Dulbecco's modified Eagle's medium (DMEM)/F-12 (Invitrogen, Carlsbad, CA, USA) contained 10% fetal bovine serum (FBS; Gbico, Carlsbad, CA, USA), 100 U/mL penicillin and 100 μg/mL streptomycin in an incubator containing 5% CO_2 at 37 °C. To mimic the inflammatory and oxidative stress conditions of PCOS, KGN cells and rat ovarian granulosa cells were inoculated with 5×10^5 cells/well in a 6-well plate and exposed to 2 mL medium (with 1% FBS) containing 10 μM lipopolysaccharide (LPS) (Beyotime, Shanghai, China) [21]. To study the effects of schisandrin, The

Dou *et al. Journal of Ovarian Research*   (2025) 18:16

Page 4 of 20

cells were treated with schisandrin at different concentrations (CAS No. HY-N0691; MedChemexpress, Shanghai, China) (0, 1.25, 2.5, 5, 10, and 20 µM) for 24 h. To investigate the effect of schisandrin on PCOS models in vitro, the cells were pretreated with 20 µM schisandrin for 24 h, followed by 10 µM LPS for 24 h. Untreated cells were used as the control.

Cell viability assay

A Cell Counting Kit-8 (CCK-8) Kit (Beyotime, Shanghai, China) was used to detect cell viability. KGN cells and rat ovarian granulosa cells were inoculated into 96-well plates at a concentration of 3×10^3 cells per well and cultured at $37°C$ overnight. Then, 10 µL of CCK-8 was added to each well of the plate. The cells were then incubated for 4 h. Next, optical density (OD) was measured at 450 nm with a microplate reader.

Reverse transcriptional quantitative polymerase chain reaction (RT-qPCR)

Total RNA was extracted from KGN cells and rat ovarian granulosa cells by TRIzol reagent (Invitrogen, Carlsbad, CA, USA) according to manufacturer's instructions. Total RNA (1 µg) was reversely transcribed using a reverse transcription kit (Takara, Dalian, China), and the cDNA was used as the qPCR template. Then, according to the manufacturer's instructions, RT-qPCR was performed on the Light Cycler 480 system using a SYBR GREEN PCR Master Mix kit (Yeasen, Shanghai, China). Aldehyde −3-phosphate dehydrogenase (GAPDH) was used as the internal reference gene, and the relative gene expression was calculated by $2^{-\triangle\triangle CT}$ method. The sequence of primers used is shown in Table 1.

Measurement of reactive oxygen species (ROS)

With 2′,7′-Dichlorodihydrofluorescein diacetate (DCFH-DA) fluorescent probe (Sigma Aldrich, Shanghai, China), intracellular ROS production was evaluated. Briefly, KGN cells and rat ovarian granulosa cells were inoculated into a 6-well plate at a density of 2×10^5 cells/well, and starved in serum-free medium for 6 h when 80–90% fusion was achieved. The cells were then incubated with a serum-free medium containing 0.1% DCFH-DA at 37 °C for 20 min in the darkness, and then washed three times with a serum-free medium. Images were captured using a BX61 fluorescence microscope (Olympus, Tokyo, Japan), and the intensity of ROS fluorescence was quantified using ImageJ software v.1.26. Superoxide dismutase (SOD) and malondialdehyde (MDA) were also detected according to the manufacturer's instructions of the corresponding detection kits (Solarbio, Beijing, China) with spectrophotometry. To detect the activity of SOD, after the cells were collected, they were weighted using a microbalance, then the cells were re-suspended with the extraction solution (10^6 cells in 1 mL of the extraction solution) and counted. Then ultrasonic decomposition was performed, and the supernatant was collected after high-speed centrifugation (8000 g, $4°C$, 10 min). After mixing the supernatant with the working solution, the sample was incubated in a water bath at 37 °C for 5 min, and the absorbance was measured at 560 nm wavelength using a spectrophotometer. At the same time, the

Table 1 Sequences of the primers used for RT-qPCR

Gene	Human	Rat
IL-1β	F: 5′-CAGAAGTACCTGAGCTCGCC-3′	F: 5′-GACTTCACCATGGAACCCGT-3′
	R: 5′-TGAAGCCCTTGCTGTAGTGG-3′	R: 5′-GGAGACTGCCCATTCTCGAC-3′
IL−6	F: 5′-ACCGGGAACGAAAGAGAAGC-3′	F: 5′-ACAGCGATGATGCACTGTCA-3′
	R: 5′-TCTCCTGGGGGGTATTGTGGA-3′	R: 5′-AGCACACTAGGTTTGCCGAG-3′
iNOS	F: 5′-GGCAGCCTGTGAGACCTTG-3′	F: 5′-ATCTTTGGCCCGAAGGTCG-3′
	R: 5′-GCATTGGAAGGAAGGAGCGTTTC-3′	R: 5′-AGTCACATGCAGCTTGTCCA-3′
PTGS2	F: 5′-GTTCCACCCGCAGTACAGAA-3′	F: 5′-ATTACTGCTGAAGCCCACCC-3′
	R: 5′-CTCCACCAAAAGTGCTTGGC-3′	R: 5′-GGCCCTGGTGTAGTAGGAGA-3′
MMP9	F: 5′-TTCAGGGAGACGCCCATTTC-3′	F: 5′-GATCCCCAGAGCGTTACTCG-3′
	R: 5′-TCGCTGGTACAGGTCGAGTA-3′	R: 5′-GTTGTGGAAACTCACACGCC-3′
MCL1	F: 5′-GCCTTCCAAGGATGGGTTTG-3′	F: 5′-AGATCATCTCCCGCTACCTG-3′
	R: 5′-AGGTTGCTAGGGTGCAACTC-3′	R: 5′-GCCCCAGTTTGTTACGCCAT-3′
JUN	F: 5′-GCCAGGTCGGCAGTATAGTC-3′	F: 5′-CCAACCAACGTGAGTGCAAG-3′
	R: 5′-GGACTCTGCCACTTGTCTCC-3′	R: 5′-GAGGGCATCGTCGTAGAAGG-3′
GAPDH	F: 5′-TCCGTGGTCCACGAGAACT-3′	F: 5′-GGACCAGGTTGTCTCCTGTG-3′
	R: 5′-GAAGCATTTGCGGTGGACGAT-3′	R: 5′-ATTCGAGAGAAGGGAGGGCT-3′

Dou *et al. Journal of Ovarian Research*   (2025) 18:16

Page 5 of 20

Table 2 Details of active compounds in *S. Rubriflora*
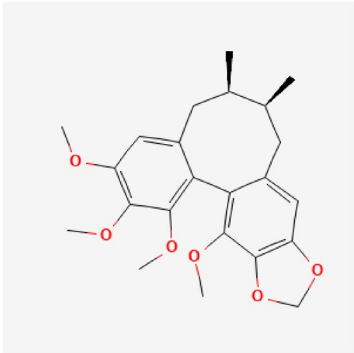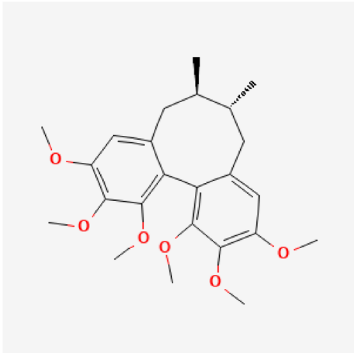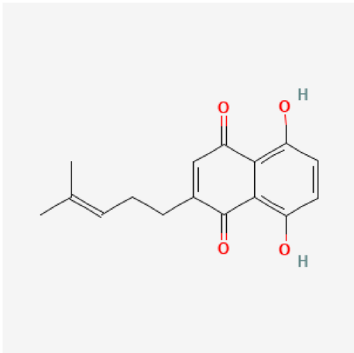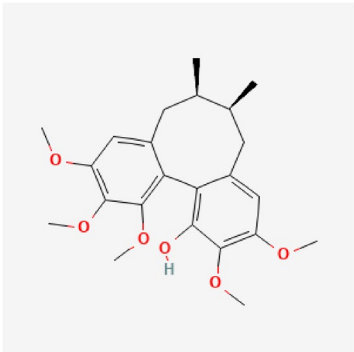
Ingredient	PubChem CID	MW (g/mol)	SMILES	Structure
Gomisin N	158,103	400.5	CC1CC2 = CC3 = C(C(= C2C4 = C(C(= C(C = C4CC1C)OC)OC)OC)OC)OCO3	
Deoxyschisandrin	10,884,218	416.5	CC1CC2 = CC(= C(C(= C2C3 = C(C(= C(C = C3CC1C)OC)OC)OC)OC)OC)OC	
Deoxyshikonin	98,914	272.29	CC(= CCCC1 = CC(= O)C2 = C(C = CC(= C2C1 = O)O)O)C	
Schisanhenol	73,057	402.5	CC1CC2 = CC(= C(C(= C2C3 = C(C(= C(C = C3CC1C)OC)OC)O)OC)OC)OC	

Dou *et al. Journal of Ovarian Research*   (2025) 18:16

Page 6 of 20

Table 2 (continued)
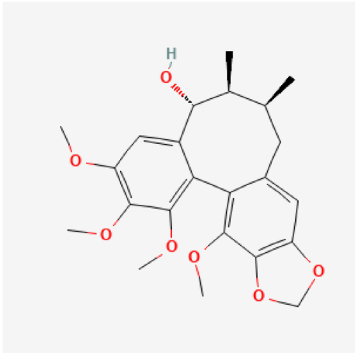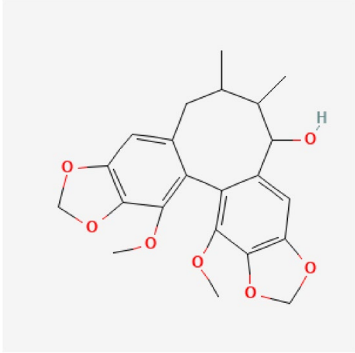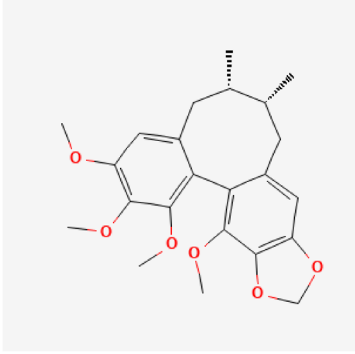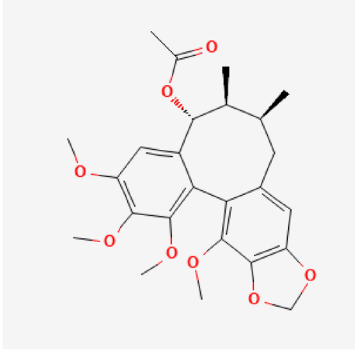
Ingredient	PubChem CID	MW (g/mol)	SMILES	Structure
Gomisin O	5,317,808	416.5	CC1CC2=CC3=C(C(=C2C4=C(C(=C(C=C4C(C1C)O)OC)OC)OC)OC)OCO3	
Gomisin R	56,660,178	400.4	CC1CC2=CC3=C(C(=C2C4=C(C5=C(C=C4C(C1C)O)OCO5)OC)OC)OCO3	
Rubschisandrin	174,277	400.5	CC1CC2=CC3=C(C(=C2C4=C(C(=C(C=C4CC1C)OC)OC)OC)OC)OCO3	
Rubschisantherin	73,353,444	458.5	CC1CC2=CC3=C(C(=C2C4=C(C(=C(C=C4C(C1C)OC(=O)C)OC)OC)OC)OC)OCO3	

Dou *et al. Journal of Ovarian Research*   (2025) 18:16

Page 7 of 20

Table 2 (continued)
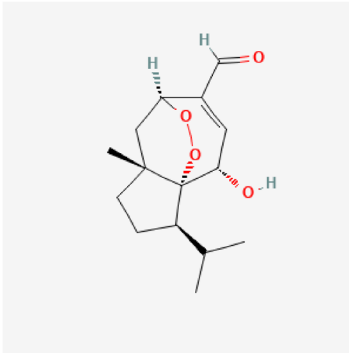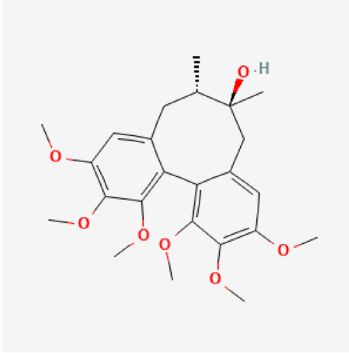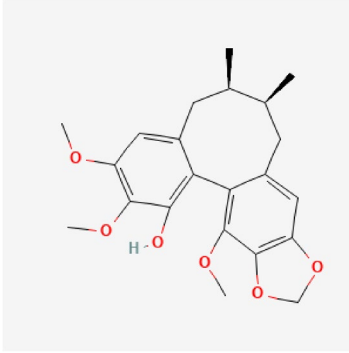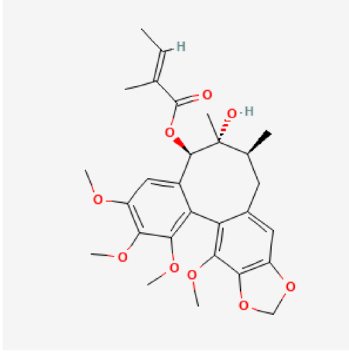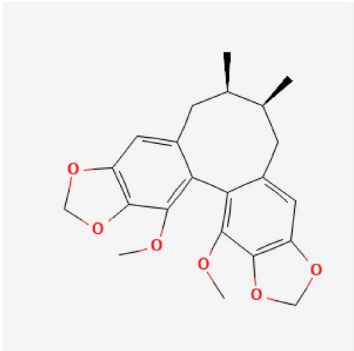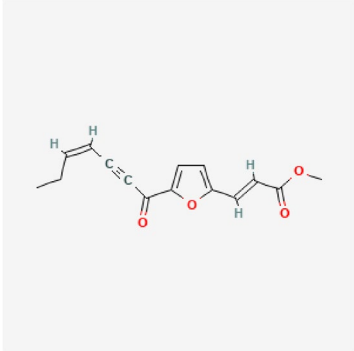
Ingredient	PubChem CID	MW (g/mol)	SMILES	Structure
Rugosal	442,391	266.33	CC(C)C1CCC2(C13C(C=C(C(C2)OO3)C=O)O)C	
Schisandrin	3,001,664	432.5	CC1CC2=CC(=C(C(=C2C3=C(C(=C(C=C3CC1(C)O)OC)OC)OC)OC)OC)OC	
Schisanhenol B	128,150	386.4	CC1CC2=CC3=C(C(=C2C4=C(C(=C(C=C4CC1C)OC)OC)O)OC)OCO3	
Tigloylgomisin P	5,318,785	514.6	CC=C(C)C(=O)OC1C2=CC(=C(C(=C2C3=C(C4=C(C=C3CC(C1(C)O)C)OCO4)OC)OC)OC)OC	

Dou *et al. Journal of Ovarian Research*   (2025) 18:16

Page 8 of 20

Table 2 (continued)

Ingredient	PubChem CID	MW (g/mol)	SMILES	Structure
Schisandrin C	443,027	384.4	CC1CC2 = CC3 = C(C(= C2C4 = C(C5 = C(C = C4CC1C) OCO5)OC)OC)OCO3	
Wyerone	643,733	258.27	CCC = CC#CC(= O)C1 = CC = C(O1)C = CC(= O)OC	

MW molecular weight

absorbance values of the control group (without working solution) and the blank group (without sample) were detected, and the inhibition rate of SOD activity in the test samples was calculated. After that, SOD activity was calculated according to the following formula: SOD activity (U/mg protein) $= 10 \times$ inhibition rate $\div (1$-percentage of inhibition$) \div$ sample weight$\times$dilution ratio. To detect MDA level, after the cells were weighted and re-suspended with the extraction solution, ultrasonic decomposition, centrifugation, mixing with working solution and incubation, the absorbance values of the samples were measured at 532 nm and 600 nm, respectively ($A532_{test}$ and $A600_{test}$). The absorbance values of a blank group (without sample) were also measured ($A532_{blank}$ and $A600_{blank}$). Then the MDA level was calculated according to the following formula: MDA level (nmol/mg protein) $= 32.258 \times [(A532_{test}$-$A532_{blank})$-$(A600_{test}$-$A600_{blank})] \div$ sample weight$\times$dilution ratio.

Apoptosis detection

An Annexin V-Fluorescein Isothiocyanate (FITC)/Propidium Iodide (PI) apoptosis detection kit (Beyotime, Shanghai, China) was used to detect apoptosis. KGN cells and rat ovarian granulosa cells were inoculated with 1×10^5 cells/well in a 6-well culture plate and incubated at 37 °C for 24 h. The cells were washed twice with a cold sterile phosphate buffered saline (PBS), and were collected and re-suspended in 100 μL of binding buffer containing 10 μL Annexin V-FITC and 5 μL PI, and stained in the dark at room temperature for 30 min. After 2 washes with PBS, cellular apoptosis was analyzed using a FACS CaliburtTM flow cytometer (BD Biosciences, Franklin Lakes, NJ, USA) within 1 h.

Western blot

RIPA lysate buffer (Beyotime, Shanghai, China) containing protease inhibitor (Roche, Mannheim, Germany) was used to lyze cells and extract total cell protein. A BCA protein detection kit (Solarbio, Beijing, China) was used to detect the protein concentration. An equal amount of protein (20 μg per sample) was separated using sodium dodecyl sulphate-polyacrylamide gel electrophoresis (SDS-PAGE) and transferred to a polyvinylidene fluoride (PVDF) membrane (Beyotime, Shanghai, China). The PVDF membrane was then blocked with 5% skim milk at room temperature for 1 h, then incubated with the primary antibodies: anti-tumor necrosis factor (TNF) receptor 1 (TNFR1) antibody (ab259817, 1:1000), anti-TNF-α antibody (ab183218, 1:1000), anti-fas cell surface death receptor (FAS) antibody (ab133619, 1:1000),
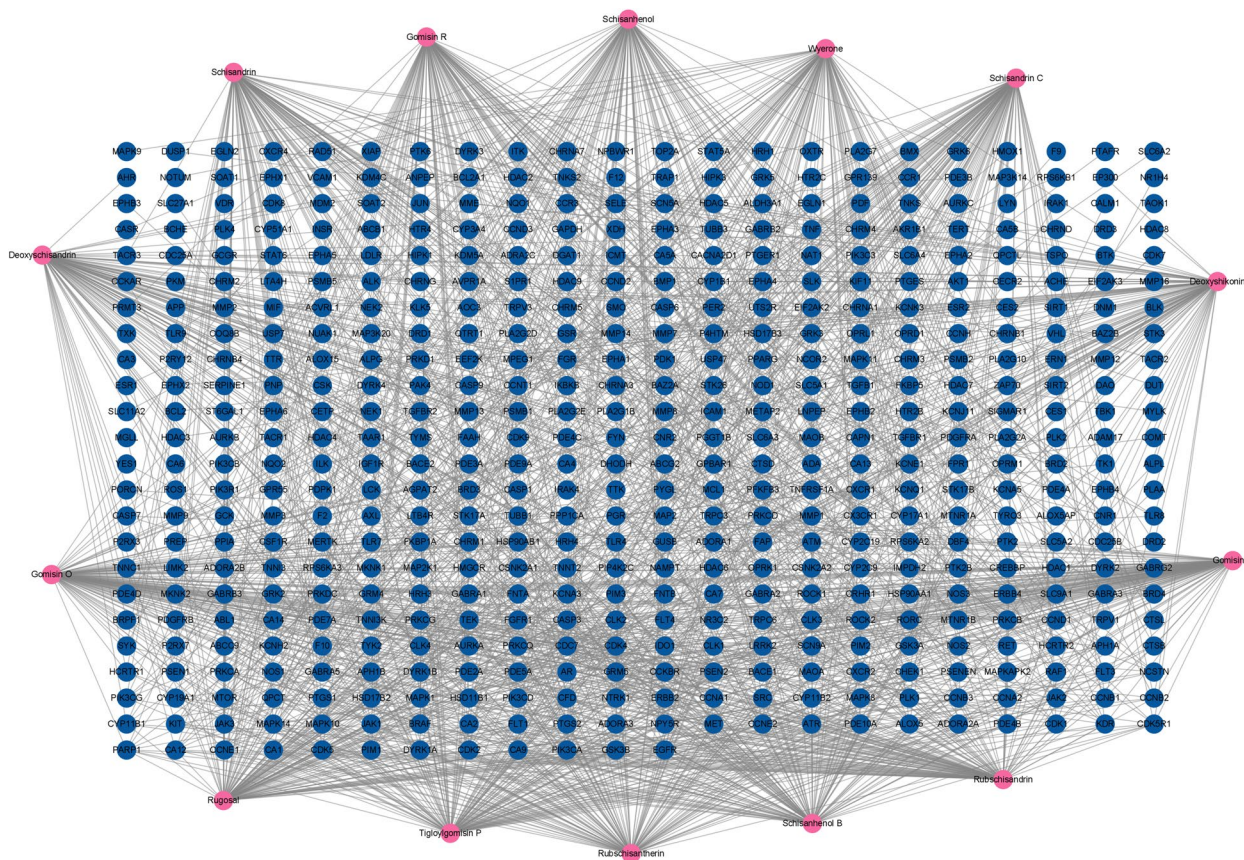
Dou *et al. Journal of Ovarian Research*   (2025) 18:16

Page 9 of 20

Fig. 1 Composition-target network of *S. rubriflora*. The pink circular nodes represent the components, and the dark blue circular nodes represent the targets

anti-Bcl-2 antibody (ab182858, 1:1000), anti-Bax antibody (ab182733, 1:1000), overnight at 4 °C. The membrane was then incubated with goat anti-rabbit IgG H&L (ab6721, 1:500) at 37 °C for 1 h. Finally, the protein bands on the membrane were developed using a BeyoECL kit (Beyotime, Shanghai, China) and quantitative analysis was performed using Image Lab™ software (Bio-Rad, Hercules, CA, USA). The antibodies used in this study were purchased from Abcam (Shanghai, China).

Statistical analysis

All experiments were conducted independently in triplicate. All data are expressed as mean ± standard deviation (SD). SPSS 21.0 software (IBM Corp., Armonk, NY, USA) was used for statistical analysis of the data. Comparisons between groups were made using Student's t-test or one-way analysis of variance (ANOVA) and Tukey *post-hoc* test. $P < 0.05$ was considered statistically significant.

Results

Identification of the targets of *S. Rubriflora* in PCOS treatment

Fourteen potential active components of *S. rubriflora* were obtained from the HERB database (Table 2). SMILES files of the components were imported into the SwissTargetPrediction database to obtain the targets of the components, and the "component-target" network was constructed using Cytoscape 3.9.0 software. As shown (Fig. 1), a network of 532 nodes and 1505 edges was obtained, which contained 518 targets of *S. rubriflora*. Next, a total of 345 DEGs were identified from GSE54248 dataset. Among them, compared with the control group, 319 genes were up-regulated and 36 genes were down-regulated in peripheral blood samples of PCOS patients (Fig. 2A). Finally, 26 common targets were obtained, which were considered as the targets of *S. rubriflora* in PCOS treatment (Fig. 2B). In addition, hierarchical cluster analysis was used to compare the expression differences of 26 common targets in peripheral blood samples of PCOS patients and control subjects. The results showed that 26
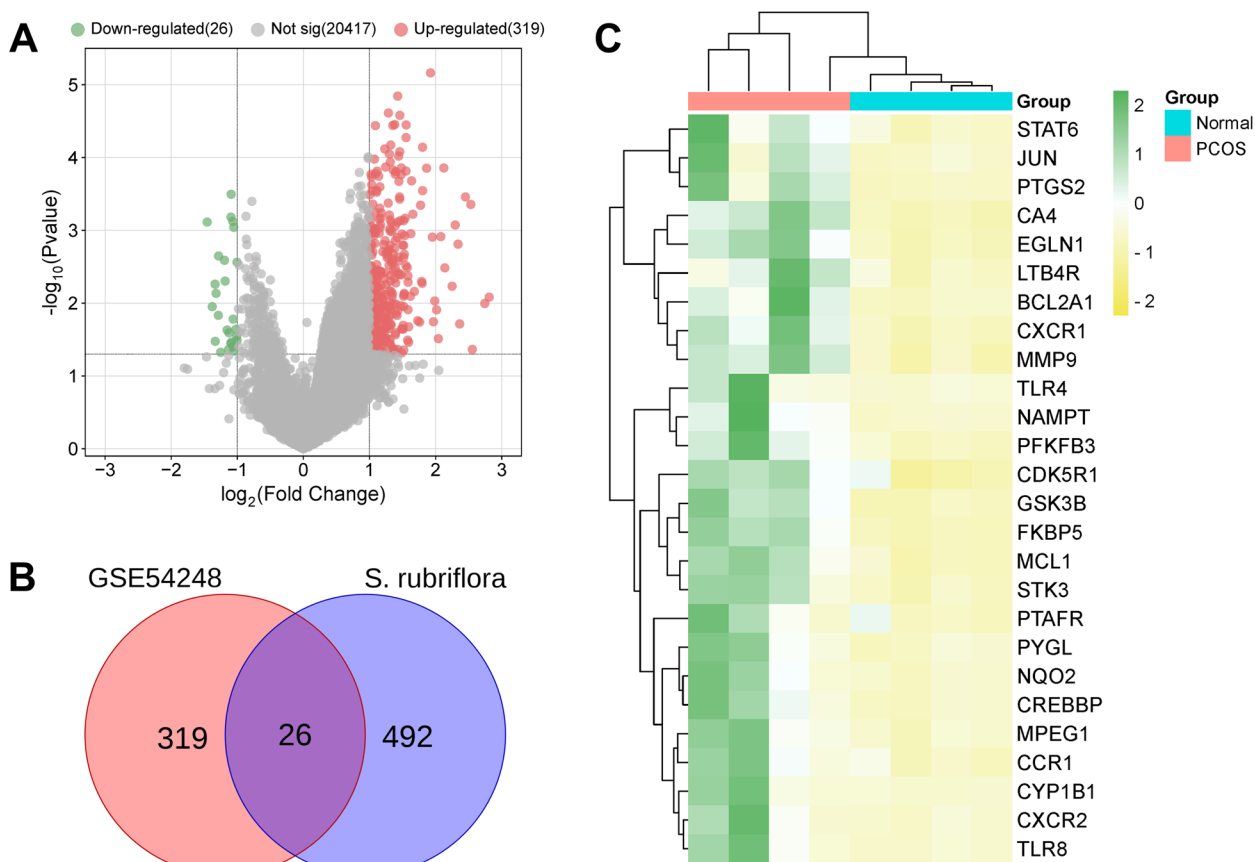
Dou *et al. Journal of Ovarian Research*   (2025) 18:16

Page 10 of 20

Fig. 2 Collection of *S. rubriflora's* targets in PCOS treatment. **A** Differential expression genes (DEGs) in peripheral blood samples of PCOS patients and control subjects were screened with $P < 0.05$, |log2 fold change|>1 as the threshold. The horizontal axis is the multiple change in gene expression, and the vertical axis is the statistical significance (*p*-value) of the change in gene expression. Pink dots represent up-regulated genes and green dots represent down-regulated genes. **B** Venn diagram of the targets of *S. rubriflora's* ingredients and the DEGs associated with PCOS. **C** Stratified clustering heat maps of the targets of *S. rubriflora* in PCOS treatment

common targets were highly expressed in PCOS compared to the control group (Fig. 2C).

Construction and analysis of PPI network

To elucidate the potential mechanism of action of *S. rubriflora* in the treatment of PCOS, 26 common targets were imported into the STRING database for PPI analysis. As shown (Fig. 3A), a network of 22 nodes and 62 edges was obtained. The average node degree of the network was 4.77, and the average local clustering coefficient was 0.584. In addition, cluster analysis using the MCODE plug-in generated a highly connected subnetwork (score=4.6) consisting of 11 nodes and 23 edges (Fig. 3B).

Functional enrichment analyses

To further explore the potential functions and mechanisms of *S. rubriflora* in PCOS treatment, GO and KEGG

pathway enrichment analyses on the 26 common targets were performed. A total of 792 GO terms were obtained ($P < 0.05$), including 689 biological processes (BP), 21 cellular components (CC), and 82 molecular functions (MF). The top 5 terms in BP were positive regulation of neuron death, positive regulation of smooth muscle cell proliferation and neuron death, neuroinflammatory response, regulation of smooth muscle cell proliferation (Fig. 4A); the top 5 terms in CC were are external side of plasma membrane, secretory granule membrane, organelle outer membrane, outer membrane, and membrane raft (Fig. 4B); the top 5 terms in MF were are C-C chemokine receptor activity, pattern recognition receptor activity, C-C chemokine binding, G protein-coupled chemoattractant receptor activity and chemokine receptor activity (Fig. 4C). In addition, KEGG analysis showed that a total of 49 pathways were associated with the 26 targets ($P < 0.05$). The top 10 pathways were Hepatitis B (hsa05161), IL-17 signaling pathway (hsa04657),
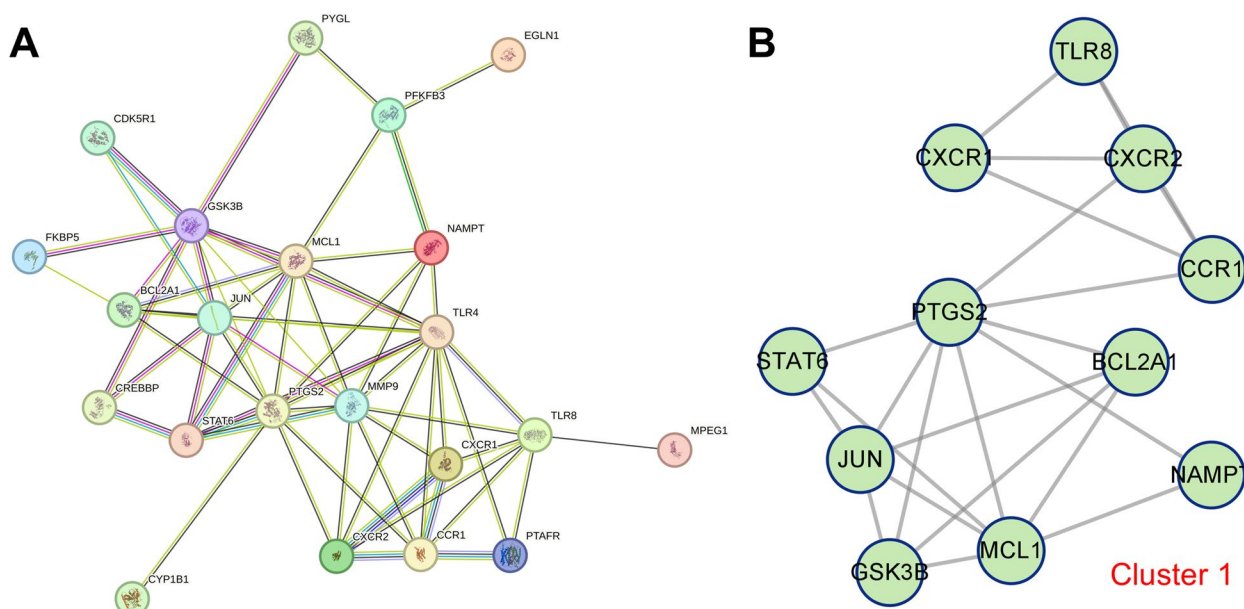
Dou *et al. Journal of Ovarian Research*   (2025) 18:16

Page 11 of 20

Fig. 3 PPI network construction and analysis. **A** PPI network of the targets of *S. rubriflora* in PCOS treatment. Nodes represent proteins and edges represent protein-protein interactions. **B** MCODE plug-in was applied to filter highly interconnected clusters in PPI network

and Kaposi sarcoma-associated herpesvirus infection (hsa05167), HIF-1 signaling pathway (hsa04066), inflammatory bowel disease (hsa05321), renal cell carcinoma (hsa05211), epithelial cell signaling in Helicobacter pylori infection (hsa05120), Leishmaniasis (hsa05140), microRNAs in cancer (hsa05206) and chemokine signaling pathway (hsa04062) (Fig. 4D).

Identification of hub targets of *S. Rubriflora* in PCOS treatment

In order to identify the hub target of *S. rubriflora* in PCOS treatment, CytoHubba plug-in was used to evaluate the PPI network (Table 3). Then, the top 10 targets of each algorithm were selected for cross analysis. The results showed that PTGS2, MMP9, MCL1 and JUN were hub targets of *S. rubriflora* in PCOS treatment (Fig. 5A). Details of these four hub targets are shown in Table 4. An additional dataset, GSE34526, was used to investigate the expression characteristics of the hub genes in human granulosa cells isolated from ovarian aspirates from healthy and PCOS women. The results showed that, except PTGS2, the expression levels of MMP9, MCL1 and JUN were markedly up-regulated in granulosa cells of the patients with PCOS, compared with the healthy controls (Supplementary Fig. 1). In addition, based on the GeneMANIA database, we constructed the gene interaction network based on the four hub targets, which was mainly related to prostaglandin biosynthesis, prostaglandin metabolism, cadmium ion reaction, arachidonic acid metabolism, and

cell response to oxidative stress (Fig. 5B). In addition, the "component-Hub target-pathway" network using Cytoscape 3.9.0 software was constructed to further explore the key components and pathways for *S. rubriflora* in PCOS treatment. As shown (Fig. 5C), the network consisted of 31 nodes and 43 edges. CytoNCA plug-in analysis showed that IL-17 signaling pathway, MicroRNAs in cancer and TNF signaling pathway were the pathways with the highest degree values in this network. Schisandrin, wyerone and rugosal were the bioactive components with the highest degree values (Table 5). The targets in the IL-17 signaling pathway and TNF signaling pathway were colored using KEGG PathView, and the hub target for *S. rubriflora* in PCOS treatment was stained with red (Fig. 5D).

Molecular docking between natural components and target proteins

To validate the results of network pharmacology, we employed molecular docking to verify the binding between hub targets to key components. As shown (Fig. 6), schisandrin could form three hydrogen bonds with GLY-135 and ASN-34 of PTGS2 protein (PDB ID: 5F19), with an affinity of −7.1 kcal/mol. Wyerone could form three hydrogen bonds with GLN-461, HIS-39 and LYS-137 of PTGS2 protein with an affinity of −7.4 kcal/mol. Rugosal could form two hydrogen bonds with SER-126, a amino acid residue of PTGS2 protein, with an affinity of −7.6 kcal/mol. Schisandrin could form two hydrogen bonds with TYR-248 and TYR-218 of MMP9
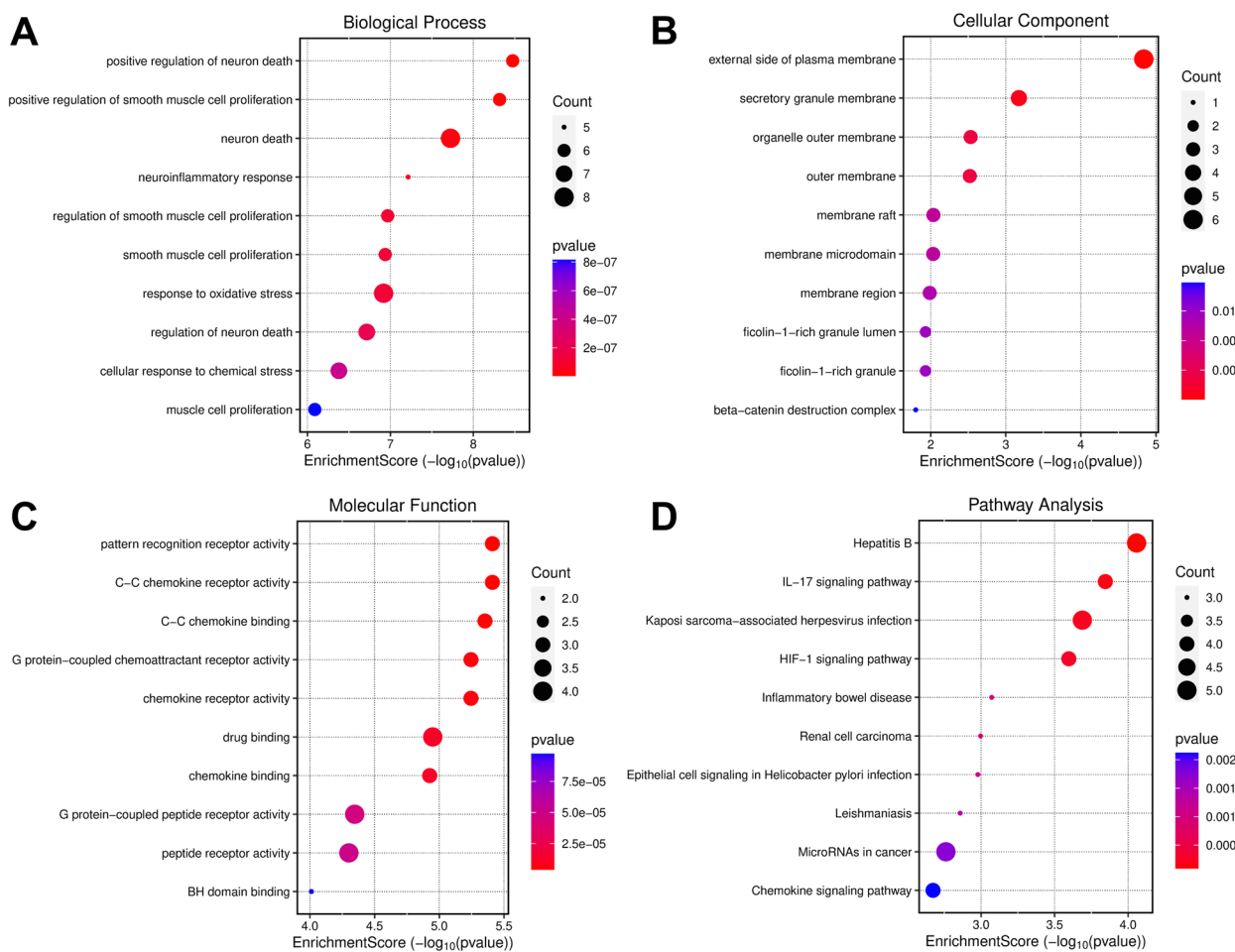
Dou *et al. Journal of Ovarian Research*   (2025) 18:16

Page 12 of 20

Fig. 4 GO and KEGG enrichment analysis of PCOS targets treated by *S. rubriflora*. **A**-**D** Bubble map of biological processes (**A**), cell components (**B**), molecular functions (**C**), and KEGG pathways (**D**) enriched by the targets of *S. rubriflora* in PCOS treatment. The bubble size represents the gene count, and the bubble color represents the *P*-value

protein (PDB ID: 6ESM) with an affinity of −5.6 kcal/mol. Wyerone could form three hydrogen bonds with GLN-227 and ARG-249 residues of MMP9 protein with an affinity of −8.1 kcal/mol. Rugosal could form three hydrogen bonds with HIS-236, HIS-226 and GLN-227 of MMP9 protein with an affinity of −6.2 kcal/mol; schisandrin could form two hydrogen bonds with SER-141 of MCL1 protein (PDB ID: 4WMS) with an affinity of −6.9 kcal/mol. Wyerone could form four hydrogen bonds with ARG-148, LYS-181 and ARG-130 of MCL1 with an affinity of −7.2 kcal/mol. Rugosal could form two hydrogen bonds with MCL1's amino acid residues GLU-43 and ASN-184 with an affinity of −8.2 kcal/mol. Schisandrin could form two hydrogen bonds with ARG-276 and ARG-279 of JUN protein (PDB ID: 5T01) with an affinity of −6.0 kcal/mol. Wyerone could form a hydrogen bond with ARG-279, an amino acid residue of JUN protein, with an affinity of −5.2 kcal/mol. Rugosal could form a hydrogen bond with LYS-283 of

JUN protein with an affinity of −4.9 kcal/mol. These results suggest high binding activity between key components and hub targets.

Schisandrin attenuated LPS-induced inflammation, oxidative stress and apoptosis of granulosa cells

To investigate the potential therapeutic effect of *S. rubriflora* on PCOS, we selected schisandrin, a key component of *S. rubriflora*, for in vitro assays. First, we examined the effects of schisandrin on the viability of KGN cells. KGN cells were treated with different concentrations of schisandrin (0, 1.25, 2.5, 5, 10, and 20 μM) for 24 h. CCK-8 assays showed that these concentrations had no significant cytotoxic effect on KGN cell viability (Fig. 7A). To determine the role of schisandrin in an i*n vitro* PCOS model, we induced inflammatory responses and oxidative stress in KGN cells using 10 μM LPS. Compared with the control group, LPS significantly reduced the viability of KGN cells (Fig. 7B). RT-qPCR showed

Dou *et al. Journal of Ovarian Research*   (2025) 18:16

Page 13 of 20

Table 3 The top 10 targets rank in cytoHubba

No.	Betweenness	Closeness	Degree	DMNC	EPC	MCC	MNC
1	TLR4	TLR4	TLR4	CXCR1	TLR4	TLR4	TLR4
2	GSK3B	MMP9	MMP9	CXCR2	PTGS2	PTGS2	MMP9
3	PTGS2	PTGS2	PTGS2	TLR8	MMP9	MMP9	PTGS2
4	MMP9	GSK3B	GSK3B	CCR1	MCL1	MCL1	JUN
5	MCL1	MCL1	JUN	MCL1	JUN	JUN	GSK3B
6	PFKFB3	JUN	MCL1	STAT6	GSK3B	GSK3B	MCL1
7	TLR8	BCL2A1	CCR1	BCL2A1	BCL2A1	CCR1	CCR1
8	JUN	CCR1	TLR8	PTGS2	CCR1	CXCR2	STAT6
9	NAMPT	STAT6	STAT6	JUN	STAT6	TLR8	TLR8
10	BCL2A1	TLR8	BCL2A1	MMP9	CXCR2	STAT6	BCL2A1
11	STAT6	CXCR2	CXCR2	PTAFR	TLR8	BCL2A1	CXCR2
12	CCR1	NAMPT	NAMPT	NAMPT	NAMPT	CXCR1	NAMPT
13	PYGL	CXCR1	CXCR1	TLR4	CXCR1	NAMPT	CXCR1
14	CXCR2	PFKFB3	PFKFB3	GSK3B	PTAFR	PTAFR	CREBBP
15	CREBBP	PTAFR	CREBBP	CREBBP	CREBBP	CREBBP	PTAFR
16	CDK5R1	CREBBP	PTAFR	CDK5R1	PFKFB3	PFKFB3	CDK5R1
17	CXCR1	PYGL	CDK5R1	PFKFB3	CDK5R1	CDK5R1	PFKFB3
18	MPEG1	CDK5R1	FKBP5	FKBP5	FKBP5	FKBP5	FKBP5
19	CYP1B1	FKBP5	PYGL	MPEG1	PYGL	PYGL	MPEG1
20	EGLN1	CYP1B1	MPEG1	CYP1B1	CYP1B1	MPEG1	CYP1B1
21	PTAFR	MPEG1	CYP1B1	EGLN1	MPEG1	CYP1B1	EGLN1
22	FKBP5	EGLN1	EGLN1	PYGL	EGLN1	EGLN1	PYGL

DMNC density of maximum neighborhood component, *EPC* edge percolated component, *MCC* maximal clique centrality, *MNC* maximum neighborhood component

that LPS stimulation significantly increased the mRNA expression levels of IL-1β, IL-6 and iNOS in KGN cells (Fig. 7C); LPS also promoted ROS and MDA production, and decreased SOD activity (Fig. 7D-F); notably, schisandrin treatment could remarkably reverse these effects (Fig. 7B-F). In addition, flow cytometry analysis showed that schisandrin treatment significantly attenuated LPS-induced apoptosis of KGN cells (Fig. 7G&H). Similarly, in rat ovarian granulosa cells, schisandrin ameliorated LPS-induced inflammation, oxidative stress and apoptosis (Supplementary Fig. 2A-H).

Schisandrin inhibits LPS-induced activation of TNF signaling pathways in KGN cells and rat ovarian granulosa cells

In order to verify whether schisandrin suppressed oxidative stress and apoptosis of KGN cells via the hub targets, RT-qPCR was performed to detect the effect of schisandrin on the mRNA expression levels of hub targets. LPS stimulation significantly upregulated mRNA expression levels of PTGS2, MMP9, MCL1, and JUN in KGN cells compared to controls, while schisandrin treatment reversed this effect (Fig. 8A-D). To further elucidate the potential mechanism of action of *S. rubriflora* in the treatment of PCOS, Western blot was applied to detect

the effect of schisandrin on the TNF signaling pathway in LPS-induced KGN cells. It showed that LPS stimulation significantly increased protein levels of TNFR1, TNF-α, and FAS in KGN cells, while schisandrin treatment significantly attenuated this effect (Fig. 8E). Similarly, in rat ovarian granulosa cells, schisandrin ameliorated LPS-induced up-regulation of PTGS2, MMP2, MCL1, JUN, TNFR1, TNF-α, and FAS (Supplementary Fig. 2A-E). These results suggest that schisandrin may play a role in the treatment of PCOS by inhibiting TNF signaling pathways by acting on targets such as PTGS2, MMP9, MCL1 and JUN.

Discussion

PCOS represents a significant contributing factor to female infertility and constitutes a substantial health concern for women globally [2]. To date, no drugs with a specific focus on PCOS have gained approval [22, 23]. Consequently, the development of novel therapeutic agents to manage PCOS is imperative. PCOS is not only related to the reproductive system, but also closely related to metabolic problems. The main treatment strategies for PCOS include oral progesterone to adjust the menstrual cycle and reduce androgen levels. Metformin is used to treat insulin resistance. For patients with fertility

Fig. 5 Identification of hub target and its related network construction. **A** 7 algorithms (betweenness, closeness, degree, EPC, MCC, DMNC and MNC) were used to identify the hub targets of *S. rubriflora* for PCOS treatment. **B** Establishment of the gene interaction network of hub targets through GeneMANIA. **C** Construction of the "Component-Hub Target-Pathway" network using Cytoscape 3.9.0 software. Dark green triangular nodes represent components, purple circular nodes represent hub targets, and blue diamond nodes represent pathways. **D** Pathview rendering of IL-17 signaling pathway and TNF signaling pathway. The hub target is marked in red

Table 4 Summary of 4 hub targets

Targets	Full name	UniProt ID	Betweenness	Closeness	Degree	DMNC	EPC	MCC	MNC
PTGS2	prostaglandin-endoperoxide synthase 2	P35354	62.59047619	15.66666667	11	0.518768202	8.003	409	10
MMP9	matrix metallopeptidase 9	P14780	52.73809524	15.83333333	11	0.492074016	7.966	408	11
MCL1	MCL1 apoptosis regulator, BCL2 family member	Q07820	48.27619048	14.83333333	9	0.52506179	7.304	386	9
JUN	Jun proto-oncogene, AP-1 transcription factor subunit	P05412	29.25238095	14.66666667	9	0.501195345	7.299	366	9

DMNC density of maximum neighborhood component, *EPC* edge percolated component, *MCC* maximal clique centrality, *MNC* maximum neighborhood component

requirements, oral drugs are used to promote ovulation. However, the clinical manifestations of PCOS vary widely, from irregular menstruation to infertility to hirsuteness and acne [3–5]. The specific combination of symptoms may be different for each patient. The challenge in treating PCOS is the variety and complexity of its symptoms and the lack of a single treatment for all symptoms. Accumulating evidence indicates that TCM may play a vital role in the management of PCOS [24–28]. In this study, we investigated the potential molecular mechanisms underpinning the therapeutic efficacy of *S. rubriflora* in treating PCOS.

Network pharmacological analysis showed that *S. rubriflora* contained 14 active ingredients, corresponding to 518 potential molecular targets. Of these, 26 targets were regarded as potential targets for *S. rubriflora* in PCOS treatment. Notably, PPI analysis based on topology parameters suggested that PTGS2, MMP9, MCL1, and JUN may be the hub targets for *S. rubriflora* in PCOS treatment. PTGS2, also known as COX-2, is a key enzyme in prostaglandin biosynthesis and is significantly highly expressed in ovarian tissue of PCOS rats

Table 5 The degree value of the "components - hub targets - pathways" network

No.	Node	Degree	No.	Node	Degree
1	PTGS2	16	17	Tigloylgomisin P	1
2	JUN	14	18	Rubschisantherin	1
3	MMP9	9	19	Gomisin R	1
4	MCL1	4	20	Gomisin O	1
5	Schisandrin	3	21	Schisanhenol	1
6	hsa04668	3	22	Deoxyshikonin	1
7	hsa05206	3	23	Deoxyschisandrin	1
8	hsa04657	3	24	hsa05135	1
9	Wyerone	2	25	hsa05163	1
10	Rugosal	2	26	hsa04620	1
11	hsa04915	2	27	hsa04064	1
12	hsa04210	2	28	hsa05215	1
13	hsa05417	2	29	hsa05120	1
14	hsa05140	2	30	hsa05211	1
15	hsa05167	2	31	hsa05321	1
16	hsa05161	2			

and testosterone-stimulated KGN cells [29]. MMP9, an important member of the matrix metalloproteinases family, is highly conserved in mammals and has been shown to be overexpressed in PCOS and involved in the pathogenesis of PCOS [30, 31]. MCL1, an anti-apoptotic member of the B-cell lymphoma 2 (BCL2) family, has been found to be significantly highly expressed in insulin-treated human granulosa tumor cells, promoting the proliferation of human granulosa tumor cells and inhibiting apoptosis [32]. JUN, also known as c-Jun, belongs to the AP-1 family of transcription factors, and c-JUN protein is significantly overexpressed in ovarian tissue of PCOS mice [33, 34]. Our data suggest that *S. rubriflora* may exert its pharmacological effects via these targets in PCOS treatment.

In this work, we established a "component-hub target-pathway" network. Remarkably, schisandrin, wyerone, and rugosal emerge as the main bioactive constituents. Notably, molecular docking hinted that high binding affinities between these constituents and the hub targets. Schisandrin, a biphenyl cycloctene lignan, exhibits hepatoprotective, anticancer, antioxidant, and anti-inflammatory properties [35]. It has been reported to be an activator of sirtuin 1 (SIRT1), a member of the class II histone deacetylase family [36]. It also ameliorates acute lung injury induced by LPS by inhibiting the NLRP3 and JAK2/STAT3 pathways [37]. Wyerone, a natural compound found in broad beans, is considered advantageous for women's health and can function as a ligand for aromatic receptors to modulate autoimmune diseases [38]. Additionally, in this work, KEGG enrichment analysis indicated that the IL-17 signaling pathway and the TNF signaling pathway were crucial for the treatment of PCOS by *S. rubriflora*. Interleukin-17 A (IL17A), a pro-inflammatory cytokine primarily secreted by T helper cells, is highly expressed in PCOS patients [39]. Tumor necrosis factor (TNF) is a cytokine with diverse biological activities, including TNF-α and TNF-β, secreted by macrophages and T lymphocytes, respectively. TNF-α is highly expressed in serum and primary cultured granulosa cells of PCOS patients [40], and is associated with insulin resistance, ovarian follicular membrane cell growth, regulation of glucose and lipid
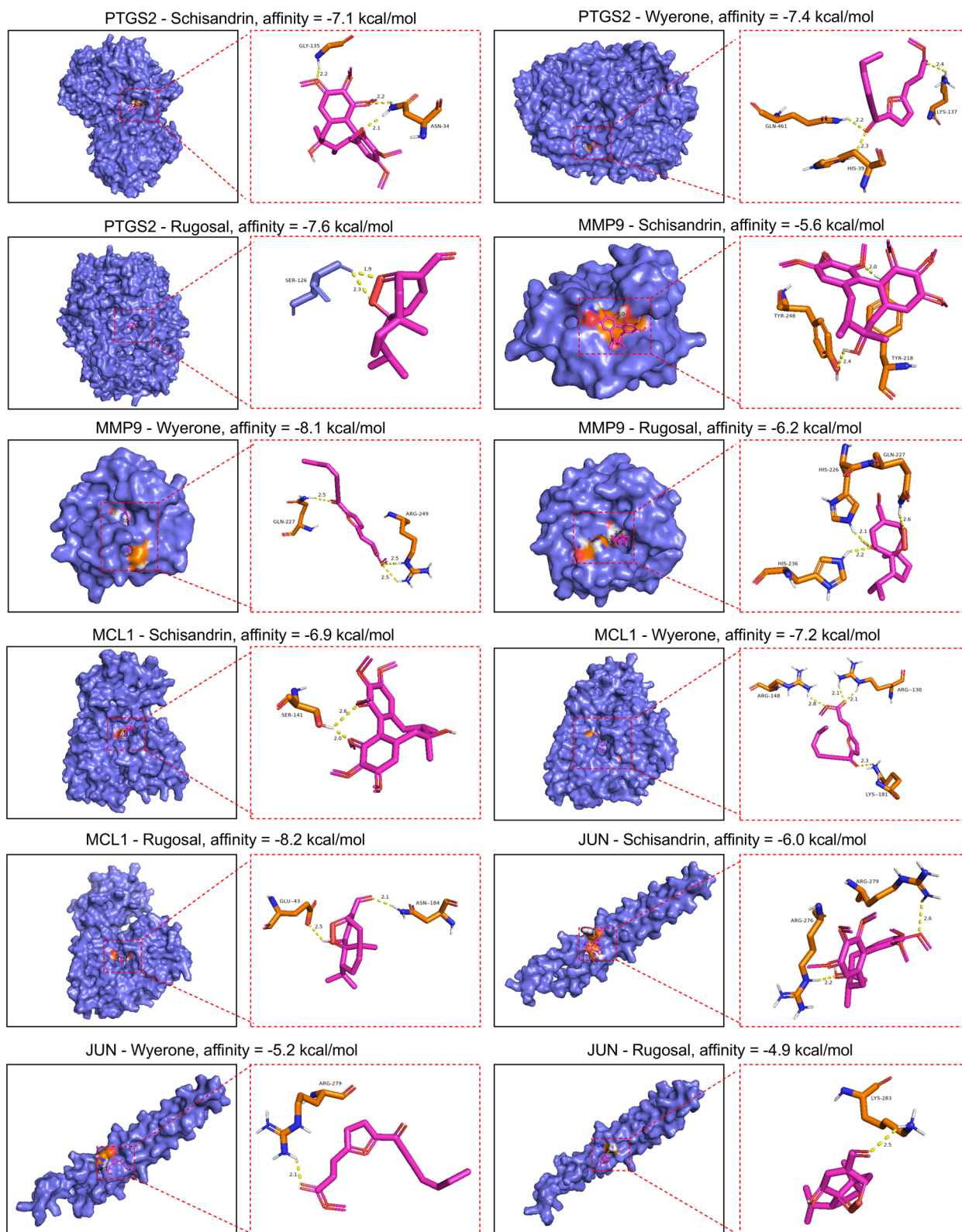
Fig. 6 3D molecular docking diagram of key components and hub targets. Pink-purple represents key components (ligands), orange represents amino acid residues around the binding pocket, and yellow dashed lines represent hydrogen bonds
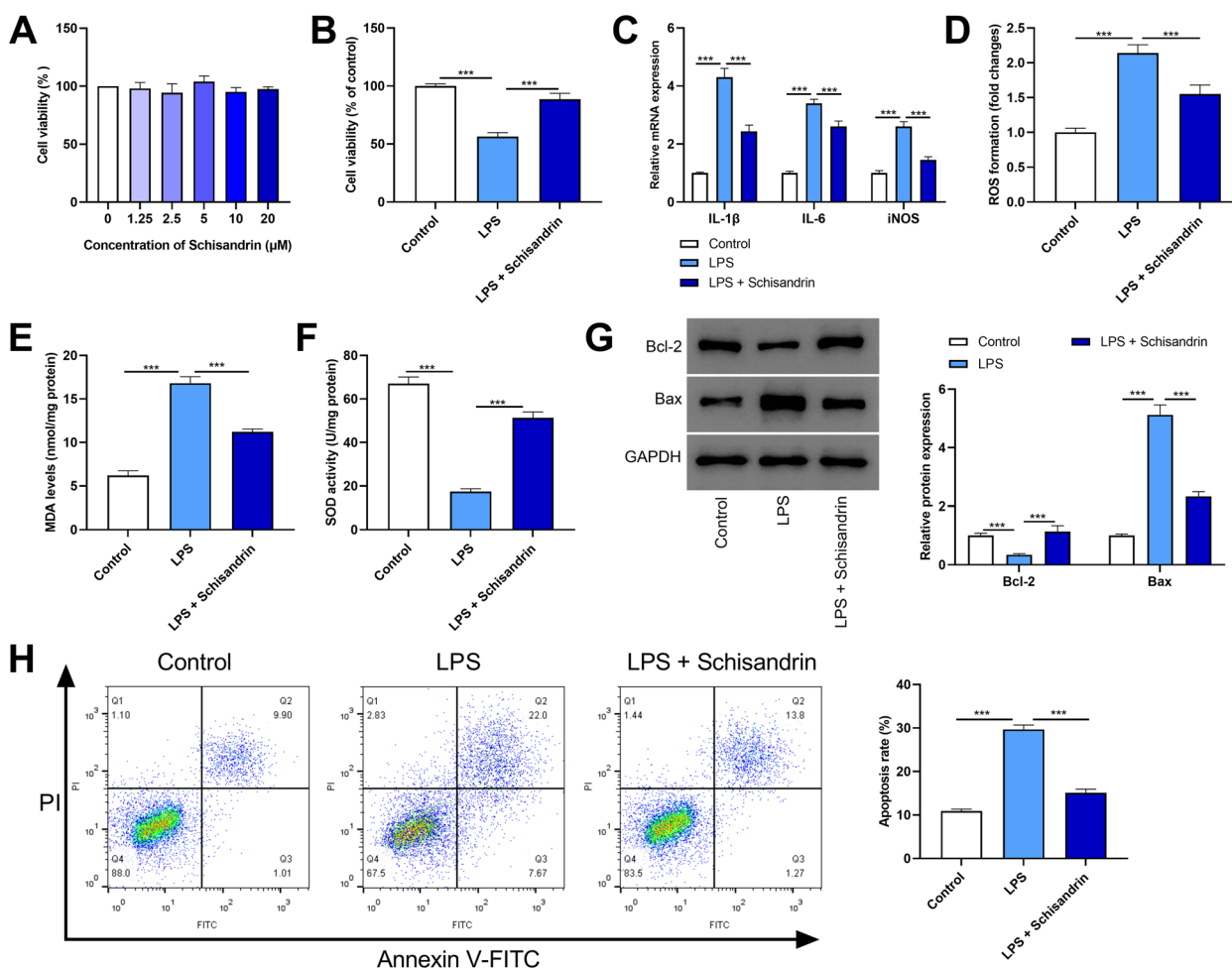
Fig. 7 Effects of schisandrin on oxidative stress and apoptosis of KGN cells induced by LPS. **A** The viability of KGN cells treated with schisandrin at different concentrations (0, 1.25, 2.5, 5, 10 and 20 μM) for 24 h was detected by CCK-8 method. **B** After being pretreated with 20 μM schisandrin and treated with 10 μM LPS for 24 h, the viability of KGN cells was detected by CCK-8 method. **C** The mRNA expression levels of IL-1β, IL-6 and iNOS in KGN cells were detected by RT-qPCR. **D**-**F** The levels of ROS, MDA and SOD were detected by the corresponding detection kit. **G** The protein expression levels of Bcl-2 and Bax were detected by Western blot. **H** Apoptosis was assessed by flow cytometry. ***, $P < 0.001$

metabolism, and steroid production [41]. Collectively, these findings suggest that *S. rubriflora* may exert therapeutic effects on PCOS through a mechanism involving multiple components, targets, and pathways.

Ovarian granulosa cells are important cells in the ovaries that support follicle development and regulate hormone secretion; apoptosis of ovarian granulosa cells may lead to oocyte apoptosis and follicular atresia, which may be one of the important factors leading to the development of PCOS [42]. Oxidative stress plays a critical role in several disorders of the reproductive system, including endometriosis, preeclampsia, and PCOS [43, 44]. Excessive ROS can damage oocytes and granulosa cells within the follicle, impairing their quality. Increased ROS level in ovarian granulosa cells induces

mitochondrial dysfunction, leads to abnormal morphology of ovarian granulosa cells, insufficient energy supply, and results in inflammation and apoptosis [44]. SOD is an important ROS clearing enzyme, and the decrease of its level indicates the enhancement of OS [45, 46]. MDA is a classic lipid peroxidation biomarker that reflects the extent of oxidative stress [44]. A 47% increase in circulating MDA levels was reported in PCOS patients compared to the control group [47]. Therefore, targeting oxidative stress and inflammation in PCOS may be a new way to prevent and treat PCOS. KGN cells have similar physiological characteristics to ovarian granulosa cells and are usually used to study the function and regulatory mechanism of granulosa cells [48]. LPS, a major component of the outer membrane of Gram-negative
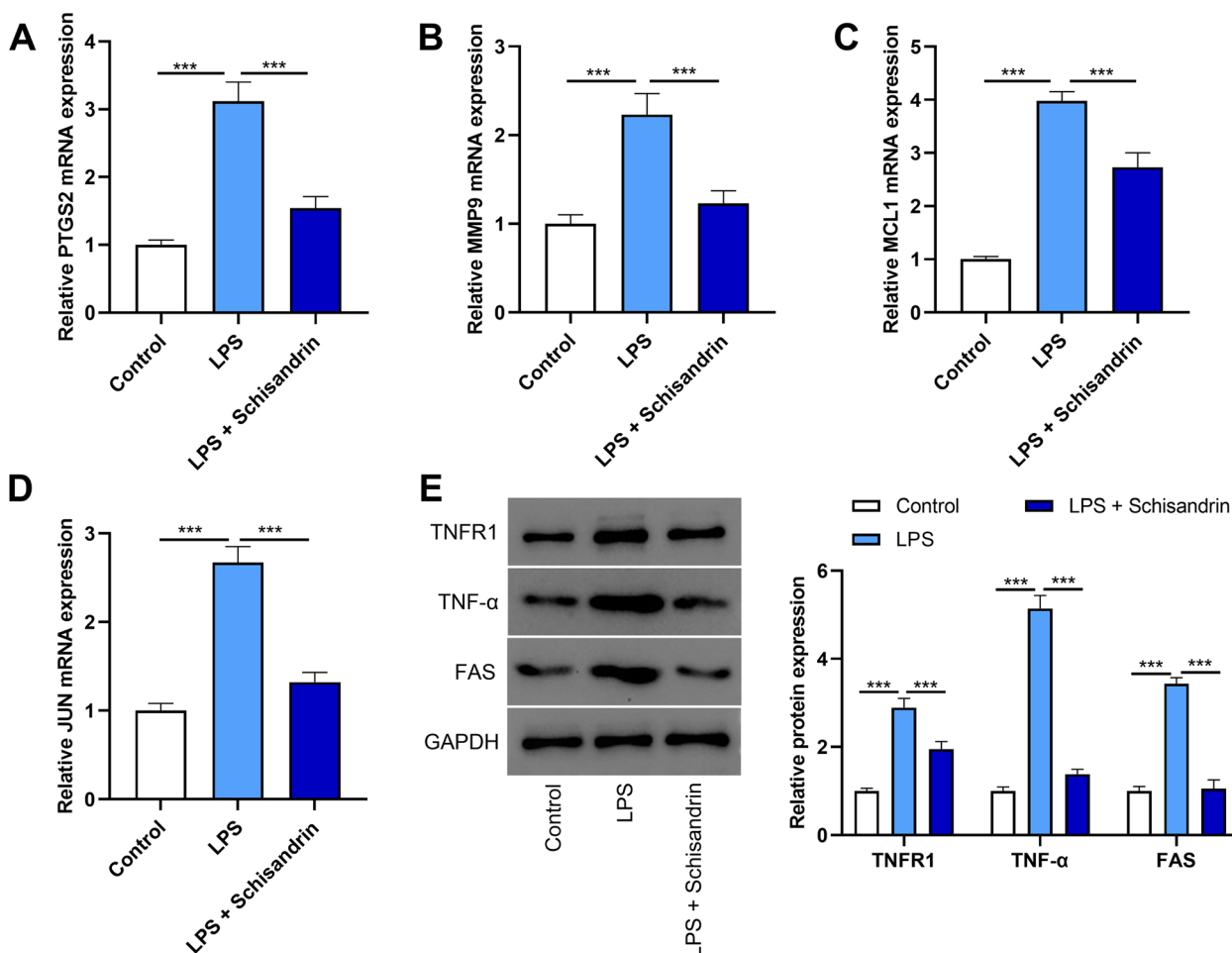
Fig. 8 Effects of Schisandrin on hub targets and TNF signaling pathway in KGN cells. **A-D** After being pretreated with 20 μM schisandrin and treated with 10 μM LPS for 24 h, the mRNA expression levels of PTGS2, MMP9, MCL1 and JUN in KGN cells were detected by RT-qPCR (**A-D**). **E** Protein expression levels of TNFR1, TNF-α and FAS were detected by Western blot. ***, $P < 0.001$

bacteria, has been widely used as an inducer of inflammation and oxidative stress in KGN cells [49, 50]. It is worth mentioning that, in this study, it was revealed that after KGN cells and rat ovarian granulosa cells were stimulated by LPS, schisandrin treatment significantly reduced ROS and MDA production, and promoted SOD activity, and repressed the production of pro-inflammatory factors IL-1β, IL-6 and iNOS. Furthermore, we found that mRNA expression levels of PTGS2, MMP9, MCL1, and JUN were significantly increased in LPS-stimulated KGN cells and rat ovarian granulosa cells, and schisandrin treatment reversed this effect. In addition, schisandrin inhibited LPS-induced activation of the TNF signaling pathway. Taken together, these findings suggest that *S. rubriflora* may play an anti-PCOS role by alleviating damage to ovarian granulosa cells through its

main active ingredient schisandrin, acting on hub targets and TNF signaling pathway.

However, it is necessary to acknowledge the limitations of this research. The findings should be verified through rigorous in vivo experimental validation. Furthermore, while schisandrin is identified as the principal active constituent, it is crucial to note that its properties do not entirely encapsulate the pharmacological activity of *S. rubriflora*. Future investigations should aim to identify and validate additional bioactive components. Additionally, the functions and molecular mechanisms underlying the potential therapeutic effects of *S. rubriflora* in PCOS require comprehensive and systematic exploration, especially its therapeutic effects on metabolic disorders.

In conclusion, therapeutic efficacy of *S. rubriflora* in PCOS treatment is primarily mediated through the modulation of key targets, including PTGS2, MMP9,

Dou *et al. Journal of Ovarian Research*   (2025) 18:16

Page 19 of 20

MCL1, and JUN. One of its main bioactive constituents, schisandrin, regulates the TNF pathway, to the mitigate inflammation, oxidative stress, and apoptosis of ovarian granulosa cells. Our work provides a theoretical basis for the application of *S. rubriflora* in PCOS treatment, as a complementary drug.

Supplementary Information

The online version contains supplementary material available at https://doi.org/10.1186/s13048-025-01600-x.

Supplementary Material 1: Supplementary Figure 1. The expression characteristics of the hub genes in human granulosa cells isolated from ovarian aspirates from healthy and PCOS women. Supplementary Figure 2. Effects of schisandrin on oxidative stress and apoptosis of rat ovarian granulosa cells induced by LPS. (A) The viability of rat ovarian granulosa cells treated with schisandrin at different concentrations (0, 1.25, 2.5, 5, 10 and 20 μM) for 24 h was detected by CCK-8 method. (B) After being pretreated with 20 μM schisandrin and treated with 10 μM LPS for 24 h, the viability of rat ovarian granulosa cells was detected by CCK-8 method. (C) The mRNA expression levels of IL-1β, IL-6 and iNOS in rat ovarian granulosa cells were detected by RT-qPCR. (D-F) The levels of ROS, MDA and SOD were detected by the corresponding detection kit. (G) The protein expression levels of Bcl-2 and Bax were detected by Western blot. (H) Apoptosis was assessed by flow cytometry. **, $P < 0.01$; ***, $P < 0.001$. Supplementary Figure 3. Effects of Schisandrin on hub targets and TNF signaling pathway in rat ovarian granulosa cells. (A-D) After being pretreated with 20 μM schisandrin and treated with 10 μM LPS for 24 h, the mRNA expression levels of PTGS2, MMP9, MCL1 and JUN in rat ovarian granulosa cells were detected by RT-qPCR (A-D). (E) Protein expression levels of TNFR1, TNF-α and FAS were detected by Western blot. **, $P < 0.01$; ***, $P < 0.001$.

Supplementary Material 2.

Supplementary Material 3.

Supplementary Material 4.

Authors' contributions
Conceived and designed the experiments: Xin Zhang; Performed the experiments: Qingxian Li1 and Zhengyan Dou; Analyzed the data: Jing Zhang and Xin Zhang; Wrote the paper: Qingxian Li, Zhengyan Dou, and Xin Zhang.All authors read and approved the final manuscript.

Data availability
No datasets were generated or analysed during the current study.

Declarations

Ethics approval and consent to participate
Not applicable.

Consent for publication
Not applicable.

Competing interests
The authors declare no competing interests.

Author details
[1]Department of Operation Room, Second Affiliated Hospital of Naval Medical University, Shanghai 200003, China. [2]Department of Reproductive Medicine Center, Second Affiliated Hospital of Naval Medical University, Shanghai 200003, China. [3]Department of Integrative Therapy, Fudan University Cancer Hospital, Shanghai 200000, China.

References
1. Siddiqui S, Mateen S, Ahmad R, Moin S. A brief insight into the etiology, genetics, and immunology of polycystic ovarian syndrome (PCOS). J Assist Reprod Genet. 2022;39(11):2439–73.
2. Deshpande PS, Gupta AS. Causes and prevalence of Factors Causing Infertility in a Public Health Facility. J Hum Reprod Sci. 2019;12(4):287–93.
3. Dapas M, Dunaif A. Deconstructing a syndrome: genomic insights into PCOS causal mechanisms and classification. Endocr Rev. 2022;43(6):927–65.
4. Escobar-Morreale HF. Polycystic ovary syndrome: definition, aetiology, diagnosis and treatment. Nat Rev Endocrinol. 2018;14(5):270–84. d.
5. Cooney LG, Dokras A. Beyond fertility: polycystic ovary syndrome and long-term health. Fertil Steril. 2018;110(5):794–809.
6. Heidarzadehpilehrood R, Pirhoushiaran M, Binti Osman M, Abdul Hamid H, Ling KH. Weighted Gene Co-expression Network Analysis (WGCNA) discovered Novel Long non-coding RNAs for polycystic ovary syndrome. Biomedicines. 2023;11(2):518.
7. Ding J, Shanshan M, Mengcheng C, Danying Z, Jin Y. Integrated Network Pharmacology and clinical study to reveal the effects and mechanisms of Bushen Huoxue Huatan Decoction on Polycystic Ovary Syndrome. Evid Based Complement Alternat Med. 2022;2022:2635375.
8. Xu D, Lu M, Liu Y, Chen W, Yang X, Xu M, Zhou H, Wei X, Zhu Y, Song Q. An analysis of the clinical medication rules of traditional Chinese medicine for polycystic ovary syndrome based on Data Mining. Evid Based Complement Alternat Med. 2023;2023:6198001.
9. Luo ED, Jiang HM, Chen W, Wang Y, Tang M, Guo WM, Diao HY, Cai NY, Yang X, Bian Y, Xing SS. Advancements in lead therapeutic phytochemicals polycystic ovary syndrome: a review. Front Pharmacol. 2023;13:1065243.
10. Nia SS, Safi F, Shoukrpour M, Kamali A. An investigation into the effect of evening primrose in dilatation of cervix and pain during and after hysterosalpingography. J Med Life. 2019;12(3):284–9.
11. Sobstyl E, Szopa A, Olszowy-Tomczyk M, Gnat S, Jafernik K, Choma IM. Chromatographic and Biological Screening of Chosen Species of Schisandraceae Family: Schisandra chinensis, S. Rubriflora, S. sphenanthera, S. Henryi and Kadsura Japonica. Chem Biodivers. 2023;20(10):e202300741.
12. Szopa A, Dziurka M, Kubica P, Jafernik K, Siomak O, Ekiert H. Stimulation of Lignan Production in Schisandra rubriflora in vitro cultures by Elicitation. Molecules. 2022;27(19):6681.
13. Jafernik K, Motyka S, Calina D, Sharifi-Rad J, Szopa A. Comprehensive review of dibenzocyclooctadiene lignans from the Schisandra genus: anticancer potential, mechanistic insights and future prospects in oncology. Chin Med. 2024;19(1):17.
14. Xiao WL, Wang RR, Zhao W, Tian RR, Shang SZ, Yang LM, Yang JH, Pu JX, Zheng YT, Sun HD. Anti-HIV-1 activity of lignans from the fruits of Schisandra rubriflora. Arch Pharm Res. 2010;33(5):697–701.
15. Szopa A, Dziurka M, Warzecha A, Kubica P, Klimek-Szczykutowicz M, Ekiert H. Targeted Lignan Profiling and Anti-inflammatory properties of Schisandra rubriflora and Schisandra chinensis extracts. Molecules. 2018;23(12):3103.
16. Jiashuo WU, Fangqing Z, Zhuangzhuang LI, Weiyi J, Yue S. Integration strategy of network pharmacology in traditional Chinese medicine: a narrative review. J Tradit Chin Med. 2022;42(3):479–86.
17. Qian Y, Yi F. Inulae Flos is a potential herbal medicine to treat glioma: a study based on gene expression profile analysis, network pharmacology and molecular docking. Diagnostics Ther. 2024;3(1):32–52.
18. Zeng Y, Xiao S, Yang L, Ma K, Shang H, Gao Y, Wang Y, Zhai F, Xiang R. Systematic analysis of the mechanism of Xiaochaihu decoction in hepatitis B treatment via network pharmacology and molecular docking. Comput Biol Med. 2021;138:104894.
19. Daina A, Michielin O, Zoete V. SwissTargetPrediction: updated data and new features for efficient prediction of protein targets of small molecules. Nucleic Acids Res. 2019;47(W1):W357–64.
20. Luo Z, Xia LY, Tang YQ, Huang L, Liu D, Huai WY, Zhang CJ, Wang YQ, Xie YM, Yin QZ, Chen YH, Zhang TE. Action mechanism underlying

improvement effect of Fuzi Lizhong Decoction on nonalcoholic fatty liver disease: a study based on Network Pharmacology and Molecular Docking. Evid Based Complement Alternat Med. 2022;2022:1670014.

21. Zhou LH, Zou H, Hao JY, Huang Y, Zhang JN, Xu XH, Li J. Metformin inhibits ovarian granular cell pyroptosis through the miR-670-3p/NOX2/ROS pathway. Aging. 2023;15(10):4429–43.

22. Shende A, Joshi S, Koli PG. Evaluation of the effects of Caesalpinia crista on Letrozole-Induced models of polycystic ovarian syndrome. Cureus. 2023;15(1):e34215.

23. Hoeger KM, Dokras A, Piltonen T. Update on PCOS: consequences, challenges, and Guiding Treatment. J Clin Endocrinol Metab. 2021;106(3):e1071–83.

24. Li X, Ullah I, Hou C, Liu Y, Xiao K. Network pharmacology and molecular docking study on the treatment of polycystic ovary syndrome with angelica sinensis- radix rehmanniae drug pair. Med (Baltim). 2023;102(46):e36118.

25. Qiu Z, Dong J, Xue C, Li X, Liu K, Liu B, Cheng J, Huang F. Liuwei Dihuang Pills alleviate the polycystic ovary syndrome with improved insulin sensitivity through PI3K/Akt signaling pathway. J Ethnopharmacol. 2020;250:111965.

26. Yu J, Liu Y, Zhang D, Zhai D, Song L, Cai Z, Yu C. Baicalin inhibits recruitment of GATA1 to the HSD3B2 promoter and reverses hyperandrogenism of PCOS. J Endocrinol. 2019;240(3):497–507.

27. Xu X, Xu X, Wang X, Shen L. Baicalin suppress the development of polycystic ovary syndrome via regulating the miR-874-3p/FOXO3 and miR-144/FOXO1 axis. Pharm Biol. 2023;61(1):878–85.

28. Sobstyl E, Szopa A, Dziurka M, Ekiert H, Nikolaichuk H, Choma IM. Schisandra Rubriflora Fruit and leaves as Promising New materials of High Biological potential: Lignan Profiling and Effect-Directed analysis. Molecules. 2022;27(7):2116.

29. Huang R, Xue X, Li S, Wang Y, Sun Y, Liu W, Yin H, Tao T. Alterations of polyunsaturated fatty acid metabolism in ovarian tissues of polycystic ovary syndrome rats. J Cell Mol Med. 2018;22(7):3388–96.

30. Ranjbaran J, Farimani M, Tavilani H, Ghorbani M, Karimi J, Poormonsefi F, Khodadadi I. Matrix metalloproteinases 2 and 9 and MMP9/NGAL complex activity in women with PCOS. Reproduction. 2016;151(4):305–11.

31. Chen Y, Ma L, Ge Z, Pan Y, Xie L. Key genes Associated with non-alcoholic fatty liver disease and polycystic ovary syndrome. Front Mol Biosci. 2022;9:888194.

32. Duan J, Cai H, Huang Y, Shi L. SNAI2-Induced CircMTO1 promotes cell proliferation and inhibits apoptosis through the miR-320b/MCL1 Axis in Human Granulosa-Like Tumor cells. Front Genet. 2021;12:689916.

33. Wernig G, Chen SY, Cui L, Van Neste C, Tsai JM, Kambham N, Vogel H, Natkunam Y, Gilliland DG, Nolan G, Weissman IL. Unifying mechanism for different fibrotic diseases. Proc Natl Acad Sci U S A. 2017;114(18):4757–62.

34. Zhang YY, Ma JX, Zhu YT, Wang YX, Chen WQ, Sun X, Zhang W, Wang CY, Ding CF. Investigation of the mechanisms and experimental verification of Cuscuta-Salvia in the treatment of polycystic ovary syndrome (PCOS) via network pharmacology. J Ovarian Res. 2022;15(1):40.

35. Zhang M, Tang Z. Therapeutic potential of natural molecules against Alzheimer's disease via SIRT1 modulation. Biomed Pharmacother. 2023;161:114474.

36. Song L, Piao Z, Yao L, Zhang L, Lu Y. Schisandrin ameliorates cognitive deficits, endoplasmic reticulum stress and neuroinflammation in streptozotocin (STZ)-induced Alzheimer's disease rats. Exp Anim. 2020;69(3):363–73.

37. Li W, Huang Q, Yu J, Yang Y, Yu J, Liu Y, Song H, Cui L, Niu X. Schisandrin improves lipopolysaccharide-induced acute lung injury by inhibiting the inflammatory response in vivo and in vitro. J Food Biochem. 2022;46(7):e14141.

38. Méndez-López LF, Sosa de León D, López-Cabanillas Lomelí M, González-Martínez BE, Vázquez-Rodríguez JA. Phytochemicals from Vicia faba beans as ligands of the Aryl Hydrocarbon Receptor to regulate Autoimmune diseases. Front Nutr. 2022;9:790440.

39. Zhai Y, Pang Y. Systemic and ovarian inflammation in women with polycystic ovary syndrome. J Reprod Immunol. 2022;151:103628.

40. Ye HY, Song YL, Ye WT, Xiong CX, Li JM, Miao JH, Shen WW, Li XL, Zhou LL. Serum granulosa cell-derived TNF-α promotes inflammation and apoptosis of renal tubular cells and PCOS-related kidney injury through NF-κB signaling. Acta Pharmacol Sin. 2023;44(12):2432–44.

41. Guan HR, Li B, Zhang ZH, Wu HS, He XL, Dong YJ, Su J, Lv GY, Chen SH. Integrated bioinformatics and network pharmacology to explore the therapeutic target and molecular mechanisms of bailing capsule on polycystic ovary syndrome. BMC Complement Med Ther. 2023;23(1):458.

42. Wang M, An K, Huang J, Mprah R, Ding H. A novel model based on necroptosis to assess progression for polycystic ovary syndrome and identification of potential therapeutic drugs. Front Endocrinol (Lausanne). 2023;14:1193992.

43. Zeber-Lubecka N, Ciebiera M, Hennig EE. Polycystic ovary syndrome and oxidative stress-from bench to Bedside. Int J Mol Sci. 2023;24(18):14126.

44. Gao Y, Zou Y, Wu G, Zheng L. Oxidative stress and mitochondrial dysfunction of granulosa cells in polycystic ovarian syndrome. Front Med (Lausanne). 2023;10:1193749.

45. Al-Gubory KH, Fowler PA, Garrel C. The roles of cellular reactive oxygen species, oxidative stress and antioxidants in pregnancy outcomes. Int J Biochem Cell Biol. 2010;42(10):1634–50.

46. Dabravolski SA, Nikiforov NG, Eid AH, Nedosugova LV, Starodubova AV, Popkova TV, Bezsonov EE, Orekhov AN. Mitochondrial dysfunction and chronic inflammation in polycystic ovary syndrome. Int J Mol Sci. 2021;22(8):3923.

47. Murri M, Luque-Ramírez M, Insenser M, Ojeda-Ojeda M, Escobar-Morreale HF. Circulating markers of oxidative stress and polycystic ovary syndrome (PCOS): a systematic review and meta-analysis. Hum Reprod Update. 2013;19(3):268–88.

48. He M, Mao G, Xiang Y, Li P, Wu Y, Zhao D, Li T. MicroRNA-664a-3p inhibits the proliferation of ovarian granulosa cells in polycystic ovary syndrome and promotes apoptosis by targeting BCL2A1. Ann Transl Med. 2021;9(10):852.

49. Yuan B, Luo S, Feng L, Wang J, Mao J, Luo B. Resveratrol regulates the inflammation and oxidative stress of granulosa cells in PCOS via targeting TLR2. J Bioenerg Biomembr. 2022;54(4):191–201.

50. Zuo T, Zhu M, Xu W, Wang Z, Song H. Iridoids with Genipin Stem Nucleus Inhibit Lipopolysaccharide-Induced inflammation and oxidative stress by blocking the NF-κB pathway in polycystic ovary syndrome. Cell Physiol Biochem. 2017;43(5):1855–65.

Publisher's Note